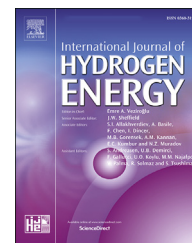




ELSEVIER

Available online at [www.sciencedirect.com](http://www.sciencedirect.com)

ScienceDirect

journal homepage: [www.elsevier.com/locate/he](http://www.elsevier.com/locate/he)

# Free convection and radiation effects in nanofluid (Silicon dioxide and Molybdenum disulfide) with second order velocity slip, entropy generation, Darcy-Forchheimer porous medium

M. Ijaz Khan <sup>a,\*</sup>, Faris Alzahrani <sup>b</sup>

<sup>a</sup> Department of Mathematics and Statistics, Riphah International University I-14, Islamabad 44000, Pakistan

<sup>b</sup> Nonlinear Analysis and Applied Mathematics (NAAM)-Research Group, Department of Mathematics, Faculty of Sciences, King Abdulaziz University, P.O. Box 80203, Jeddah, 21589, Saudi Arabia

## HIGHLIGHTS

- Here mixed convective entropy optimized flow of viscous material is addressed.
- Flow is saturated via Darcy-Forchheimer porous medium.
- Total entropy rate is calculated through second law of thermodynamics.
- Two different types of hybrid nanofluid are considered.

## ARTICLE INFO

### Article history:

Received 28 April 2020

Received in revised form

16 July 2020

Accepted 27 September 2020

Available online xxx

### Keywords:

Second order velocity slip

Entropy generation

Darcy-Forchheimer porous medium

Convective boundary condition

Thermal radiation

## ABSTRACT

In this research, communication, mathematical modeling and numerical simulation are presented for the steady, incompressible two-dimensional Darcy-Forchheimer nanofluid flow of viscous material towards a stretched surface. The flow is generated due to stretching surface and saturated through Darcy-Forchheimer relation. The radiative heat flux and viscous dissipation effects are utilized in the modeling of energy expression. Second order slip and convective condition are imposed at the stretchable boundary for velocity and temperature respectively. A total entropy rate, which depends three different types of irreversibilities i.e., heat transfer, fluid friction and Darcy-Forchheimer relation or porosity are calculated via the second law of thermodynamics. Here Silicon dioxide and Molybdenum disulfide are considered as nanomaterials and water as base fluid. The boundary layer approximation concept is used to model the governing equations of momentum and temperature. Appropriate similarity transformations are used to alter the governing equations into ordinary ones and numerical results are obtained via Built-in-Shooting method. The obtained results are compared with existing work and noticed to be in excellent agreement. Behavior of pertinent flow parameters is discussed graphically on the velocity, temperature, Bejan number and entropy generation for both nanoparticles (Silicon dioxide, Molybdenum). Furthermore, the skin friction coefficient (surface drag

\* Corresponding author.

E-mail address: [mikhan@math.qau.edu.pk](mailto:mikhan@math.qau.edu.pk) (M.I. Khan).

<https://doi.org/10.1016/j.ijhydene.2020.09.240>

0360-3199/© 2020 Hydrogen Energy Publications LLC. Published by Elsevier Ltd. All rights reserved.

force) and heat transfer rate (Nusselt number) are discussed in the presence of slip parameters and stratification parameter. It is noted from the obtained results that entropy generation rate enhances for higher Brinkman number and temperature decreases against higher values of stratification parameter.

© 2020 Hydrogen Energy Publications LLC. Published by Elsevier Ltd. All rights reserved.

## Introduction

Entropy generation minimization (EGM) have wide range of applications in heat transfer and fluid mechanics. EGM is done to improve and optimize the flow regime along with operating conditions to get the better results and to enhance the performance of operating system. In case of microsystems the condition is very complicated because the entropy is generated due to heat transfer and the flow of viscous fluid which causes heat dissipation. In some systems, recent studies shows that EGM treat the operating system as a black box. EGM leads the system towards irreversibility which in turn optimize the system. Numerous researchers and analysts are focused on boundary layer and stretched flow with entropy generation in the past couple of years [1–7].

The recent research is being done on the generation of entropy due to convective heat transfer. Many scientists and researchers did research on it to study the amount of entropy generated in the process of convection. Initially the concept of minimization of entropy was presented by the scientists which then used in heat transfer apparatuses as an optimization instrument. He studied that in convective heat transfer systems the irreversibility of thermodynamic system depends on fluid flow regime, geometry of the system and its physical characteristics. The EGM technique was the used in other conditions and systems as well. Refs. [8–14] are recently focused on the study of entropy optimization in the presence of convective heat transfer i.e., free or mixed convection.

Heat transfer is used in various industries. Heat transfer is either done from the system to the system and it is important task in any industrial facility. These systems provide heat recovery in the industrial system which makes it economical and enhance the life of the equipment. Many methods are proposed to enhance the capability of heat transfer. One of them is to enhance the thermal conductivity of the fluid. Water, engine oil and ethylene glycol are common heat transfer fluids but their thermal conductivity is very low as compared to the solids but we can increase the thermal conductivity of the fluid by using solid particles which have high thermal conductivity of the fluid. These solids particles are previously investigated by several researchers with size 2 millimeters or micrometers but it has some flaws such as (i) particles are so heavy that they immediately starts settling on the surface and starts decreasing the capacity of heat transfer. (ii) When circulation of the fluid enhances sedimentation will be decay but erosion factor drastically increases in pipelines, heat transfer devices etc. (iii) Also when size of the particles is

large clogging starts in the flow channels especially when cooling channels are small. (iv) Pressure drop increases very drastically. Thus due to all these reasons suspension of solid particles in liquid is a well-known phenomenon but it is useless for heat transfer applications. After the modern technology now we are capable to make a nanometer-sized particles which are very much different and useful. Nanofluid is a modern heat transfer mechanism having nanoparticles (1–100 nm) which are suspended in a base fluid. Material of these nanoparticles is commonly metal oxide or metal which use to increase the thermal conductivity, convection and conduction consequently heat transfer enhances [15–25].

In the present communication, mixed convective Darcy-Forchheimer second order velocity slip flow of viscous material with entropy generation is simulated numerically. The flow is generated due to stretching surface and saturated through Darcy-Forchheimer relation. The energy equation is modeled subject to radiative heat flux and dissipation. Molybdenum disulfide and silicon dioxide are taken for nanoparticles and water for base fluid. Total entropy rate which depends on three different types of irreversibilities i.e., heat transfer, fluid friction and porosity are calculated through second law of thermodynamics. Numerical results are obtained via Built-in-Shooting method and compared with Shiaq et al. [26], Wang [27] and Golra and Sidawi [28] and found good agreement with them.

## Statement

Here mathematical modeling is presented for the steady, incompressible 2D convective flow of nanofluid towards a stretched surface is addressed. The flow is caused due to stretching surface and saturated through Darcy-Forchheimer porous medium. Two different types of nanoparticles i.e., Silicon dioxide and molybdenum disulfide are considered and water as a continuous phase fluid. Furthermore, viscous dissipation, heat source/sink and radiative heat flux effects are considered for the modeling of energy expression. Let us assumed that  $u = U_w = cx + \lambda_1 \left( \frac{\partial u}{\partial y} \right) + \lambda_2 \left( \frac{\partial^2 u}{\partial y^2} \right)$  highlights the stretching velocity in the x-direction with second order velocity slip. Also,  $T_w$ ,  $T_\infty$  denotes the wall temperature and ambient temperature respectively. The desired governing equations are

**Table 1 – Thermophysical properties of nanomaterials.**

Characteristics	Nanomaterials
Density	$\rho_{nf} = \rho_f \left( 1 - \phi + \phi \frac{\rho_s}{\rho_f} \right)$ ,
Viscosity	$\mu_{nf} = \frac{\mu_f}{(1 - \phi)^{2.5}}$ ,
thermal conductivity	$\frac{k_{nf}}{k_f} = \frac{k_s + 2k_f - 2\phi(k_f - k_s)}{k_s + 2k_f + 2\phi(k_f - k_s)}$ ,
heat capacity	$(\rho c_p)_{nf} = (\rho c_p)_f \left( 1 - \phi + \phi \frac{(\rho c_p)_s}{(\rho c_p)_f} \right)$

$$\frac{\partial u}{\partial x} + \frac{\partial v}{\partial y} = 0, \tag{1}$$

$$u \frac{\partial u}{\partial x} + v \frac{\partial u}{\partial y} = \frac{\mu_{nf}}{\rho_{nf}} \frac{\partial^2 u}{\partial y^2} - \frac{\mu_{nf}}{\rho_{nf}} \frac{1}{k_p} u - F u^2, \tag{2}$$

$$u \frac{\partial T}{\partial x} + v \frac{\partial T}{\partial y} = \frac{k_{nf}}{(\rho c_p)_{nf}} \frac{\partial^2 T}{\partial y^2} + \frac{\mu_{nf}}{(\rho c_p)_{nf}} \left( \frac{\partial u}{\partial y} \right)^2 + \frac{\mu_{nf}}{k_p (\rho c_p)_{nf}} u^2 - \frac{16 \sigma^* T_\infty^3}{3 k^* (\rho c_p)_{nf}} \frac{\partial^2 T}{\partial y^2} + \frac{Q_0}{(\rho c_p)_{nf}} (T - T_\infty), \tag{3}$$

$$u = U_w = cx + \lambda_1 \left( \frac{\partial u}{\partial y} \right) + \lambda_2 \left( \frac{\partial^2 u}{\partial y^2} \right), \quad v = 0, \quad T = T_w, \quad \text{at } y = 0, \tag{4}$$

$$u = 0, \quad T = T_\infty, \quad \text{at } y = \infty.$$

Note that  $x, y$  represent the Cartesian coordinates,  $\mu_{nf}$  the dynamic viscosity,  $u, v$  the velocity components,  $\rho_{nf}$  the density,  $k_p$  permeability,  $T$  the temperature,  $F \left( = \frac{C_b}{\alpha k_p^{1/2}} \right)$  the non-uniform inertia coefficient,  $k_{nf}$  the thermal conductivity,  $C_b$  the drag force,  $c_p$  the specific heat,  $\sigma^*$  the Stefan -Boltzman constant,  $Q_0$  the coefficient of heat source/sink,  $k^*$  the mean absorption coefficient,  $T_\infty$  the ambient temperature,  $U_w$  the stretching velocity,  $c$  the dimensional constant,  $\lambda_1 > 0$  and  $\lambda_2 < 0$  are first and second order slip coefficients and  $T_w$  the wall temperature.

Tables 1 and 2 denotes the thermophysical and transport properties of nanomaterials and continuous phase fluid. In these Tables,  $nf, s$  and  $\phi$  stand for nanofluids, nano-solid particles and nanoparticles volume fraction.

Considering

**Table 2 – Thermophysical characteristics of specific heat, thermal conductivity and density of base fluid water (H<sub>2</sub>O), Silicon dioxide (SiO<sub>2</sub>) and Molybdenum disulfide (MoS<sub>2</sub>).**

Transport characteristics	Silicon dioxide (SiO <sub>2</sub> )	Water (H <sub>2</sub> O)	Molybdenum disulfide (MoS <sub>2</sub> )
$\rho$ (kg /m <sup>3</sup> )	2650	997.1	5060
$k$ (W /mK)	1.5	0.613	34.5
$c_p$ (J /kgK)	730	4179	397.746

$$u = cx f'(\eta), \quad v = -\sqrt{cx} f(\eta), \quad \theta(\eta) = \frac{T - T_\infty}{T_w - T_\infty}, \quad \eta = \sqrt{\frac{c}{\nu_f}} y. \tag{5}$$

We arrive

$$f''' - \lambda f' - A_1^* (f'^2 - ff'') - A_1^* F_0 f' = 0, \tag{6}$$

$$A_3^* \theta'' + Rd \theta'' + A_2^* Pr f \theta' + \frac{Br}{(1 - \phi)^{2.5}} f'^2 + \frac{Br \lambda}{(1 - \phi)^{2.5}} f'^2 + \beta Pr \theta = 0, \tag{7}$$

$$f(0) = 0, \quad f'(0) = 1 + L_1 f''(0) + L_2 f'''(0), \quad \theta(0) = 1, \quad f'(\infty) = 0, \quad \theta(\infty) = 0. \tag{8}$$

Note that  $\lambda, F_0, Rd, Pr, \beta, L_1, L_2, Ec$  and  $Br$  highlight the porosity parameter, inertia coefficient, radiation parameter, Prandtl number, heat generation/absorption parameter, first, second order slip parameters, Eckert number and Brinkman number.

Mathematically these variables are

$$\left. \begin{aligned} \lambda \left( = \frac{\nu_f}{ck_p} \right), F_0 \left( = \frac{C_b}{k_p^{1/2}} \right), Rd \left( = \frac{16 \sigma^* T_\infty^3}{3 k^* k_f} \right), Pr \left( = \frac{\nu_f}{\alpha_f} \right), \beta \left( = \frac{Q_0}{c(\rho c_p)_f} \right), \\ L_1 \left( = \lambda_1 \sqrt{\frac{c}{\nu_f}} \right), L_2 \left( = \lambda_2 \left( \frac{c}{\nu_f} \right) \right), Ec \left( = \frac{(cx)^2}{c_p(T_w - T_\infty)} \right), Br \left( = Ec Pr \right). \end{aligned} \right\} \tag{9}$$

Also,  $A_1^*, A_2^*$  and  $A_3^*$  are addressed as

$$\left. \begin{aligned} A_1^* &= (1 - \phi)^{2.5} \left( 1 - \phi + \phi \frac{\rho_s}{\rho_f} \right), \\ A_2^* &= \left( 1 - \phi + \phi \frac{(\rho c_p)_s}{(\rho c_p)_f} \right), \\ A_3^* &= \frac{k_{nf}}{k_f} = \frac{k_s + 2k_f - 2\phi(k_f - k_s)}{k_s + 2k_f + 2\phi(k_f - k_s)}. \end{aligned} \right\} \tag{10}$$

### Modeling of entropy generation

Mathematically, entropy generation in presence of Darcy-Forchheimer porous medium is addressed as

$$S_G = \frac{k_f}{T_\infty^2} \left( \frac{k_{nf}}{k_f} + \frac{16 \sigma^* T_\infty^3}{3 k^* k_f} \right) \left( \frac{\partial T}{\partial y} \right)^2 + \frac{\mu_{nf}}{T_\infty} \left( \frac{\partial u}{\partial y} \right)^2 + \frac{\mu_{nf}}{T_\infty k_p} u^2, \tag{11}$$

in dimensionless form, it is defined as

$$N_G = \alpha Re (A_3^* + Rd) \theta'^2 + \frac{Br Re}{(1 - \phi)^{2.5}} f'^2 + \frac{Br Re \lambda}{(1 - \phi)^{2.5}} Br f'^2. \tag{12}$$

The Bejan number which is the ratio of heat and mass transport to total entropy is addressed as

$$Be = \frac{\text{Heat transfer irreversibility}}{\text{Total entropy}}, \tag{13}$$

where  $Br \left( = \frac{\mu_f (cx)^2}{k_f (T_w - T_\infty)} \right)$ ,  $N_G \left( = \frac{S_G x^2 T_\infty}{k_f (T_w - T_\infty)} \right)$ ,  $\alpha \left( = \frac{(T_w - T_\infty)}{T_\infty} \right)$  and  $Re \left( = \frac{cx^2}{\nu_f} \right)$  signify the Brinkman number, entropy generation rate, temperature difference parameter and Reynold number.

**Table 3 – Comparative analysis of heat transport with Shiaq et al. [26], Golra and Sidawi [27] and Wang [28] when  $\phi = \lambda = Br = \beta = Rd = 0$ .**

Pr	Shiaq et al. [26]	Golra and Sidawi [27]	Wang [28]	Obtained results
0.07	0.0656	0.0656	0.0656	0.0663
0.20	0.1691	0.1691	0.1691	0.1688
0.70	0.4539	0.4539	0.4539	0.4579
2.00	0.9114	0.9114	0.9114	0.9119
7.00	1.8954	1.8954	1.8954	1.8994
20.00	3.3539	3.3539	3.3539	3.3533
70.00	6.4622	6.4622	6.4622	6.4629

**Engineering curiosity**

Mathematically, the coefficient of skin friction ( $C_{fx}$ ) and Nusselt number ( $Nu_x$ ) are defined as

$$\left. \begin{aligned} C_{fx} &= \frac{\tau_w|_{y=0}}{\rho_f (U_w)^2}, \\ Nu_x &= \frac{xq_w|_{y=0}}{k_f (T_f - T_\infty)}, \end{aligned} \right\} \quad (14)$$

where ( $\tau_w$ ) and ( $q_w$ ) are addressed as

$$\left. \begin{aligned} \tau_w &= \mu_{nf} \frac{\partial u}{\partial y}, \\ q_w &= -k_{nf} \frac{\partial T}{\partial y} - \frac{16}{3} \frac{\sigma^* T_\infty^3}{k^*} \frac{\partial T}{\partial y}. \end{aligned} \right\} \quad (15)$$

Finally, we arrive to the following form

$$\left. \begin{aligned} C_{fx} Re_x^{1/2} &= \frac{1}{(1-\phi)^{2.5}} f''(0), \\ Nu_x &= -(A_3^* + Rd) \theta'(0), \end{aligned} \right\} \quad (16)$$

in which  $Re_x^{0.5} \left( = \frac{U_w x}{\nu_f} \right)$  highlights the local Reynold number.

**Comparative analysis**

The obtained outcomes are compared with published ones i.e., Shiaq et al. [26], Golra and Sidawi [27] and Wang [28] and noticed to be an excellent agreement. For this purpose Table 3 is sketched to validate the present results with Shiaq et al. [26], Wang [27] and Golra and Sidawi [28]. It is noticed from Table 3, the results are very good with previous ones.

**Physical description**

In this section built in shooting method of Newton is employed to find the numerical solution for nonlinear differential system. Here we will discuss for both nanofluids ( $SiO_2$  – water and  $MoS_2$  – water) the impact of valuable parameters on Bejan number, entropy generation, velocity, temperature, skin friction and Nusselt number.

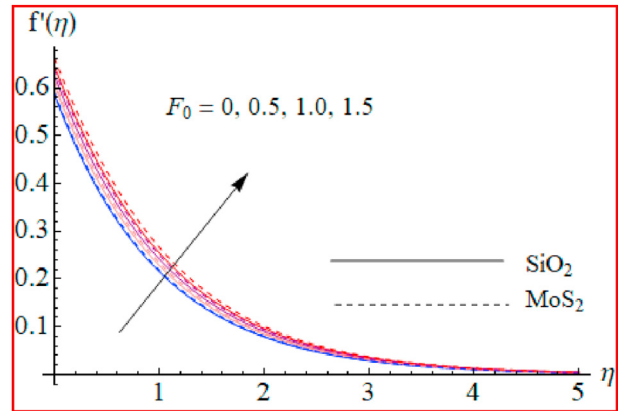


**Fig. 1 –  $F_0$  versus  $f'(\eta)$ .**

**Velocity**

Impact of Darcy Forchheimer number ( $F_0$ ), volume fraction coefficient ( $\phi$ ) and first and second order slip parameter on velocity of  $SiO_2$  – water and  $MoS_2$  – water is seen in Figs. (1-4). Fig. 1 analyzes that velocity of the fluid starts increasing with higher estimations of ( $F_0 = 0, 0.5, 1.0, 1.5$ ) due to increase in

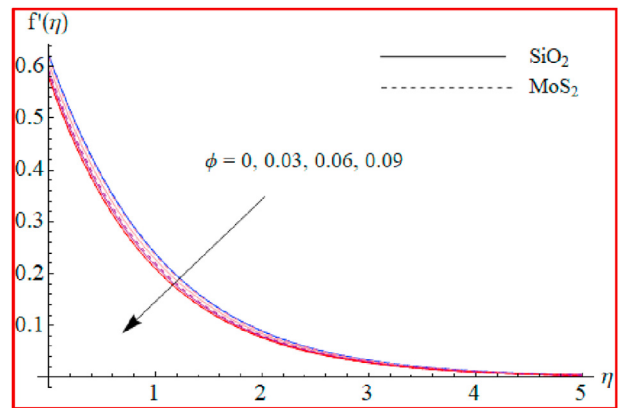


**Fig. 2 –  $\phi$  versus  $f'(\eta)$ .**

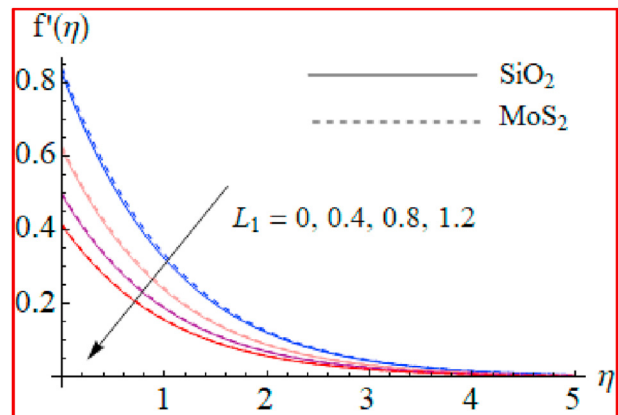


**Fig. 3 –  $L_1$  versus  $f'(\eta)$ .**

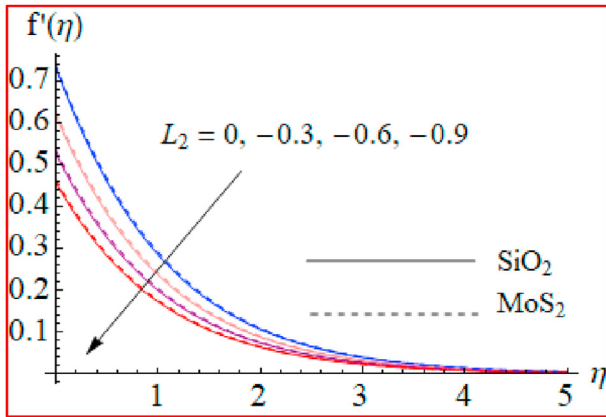


Fig. 4 –  $L_2$  versus  $f'(\eta)$ .

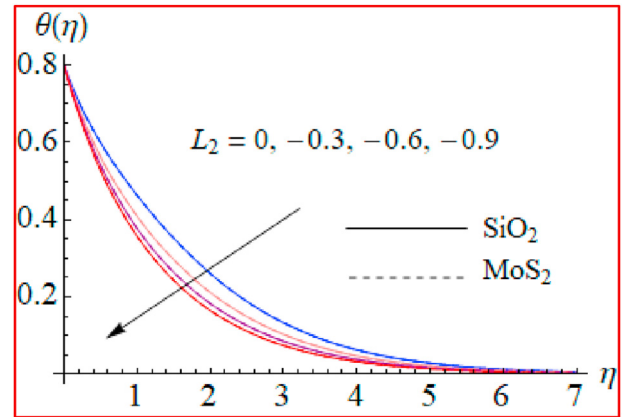


Fig. 7 –  $L_2$  versus  $\theta(\eta)$ .

disturbance through inertia coefficient. One can see that velocity of MoS<sub>2</sub> is more as compared to SiO<sub>2</sub>. Fig. 2 is plotted to show the behavior of  $(f'(\eta))$  against larger  $(\phi)$ . One can easily see that velocity decays with increasing  $(\phi)$ . It is happening because for higher  $(\phi)$  there exist more nanoparticles in the fluid due to which resistance increases hence velocity decays for both nanofluids. Figs. 3 and 4 discuss the effect of first ( $L_1$ ) and second order slip parameters ( $L_2$ ) on  $(f'(\eta))$ . When we increase slip parameters velocity of the surface and particles

attached to the surface is different due to which stretching effects are partially transfer to the fluid that is why velocity decays.

Temperature

Influence of thermal stratification parameter ( $S_1$ ), first order slip parameter ( $L_1$ ) and second order slip parameter ( $L_2 < 0$ ) against temperature field is seen in Figs. (5-7). Fig. 5 reveals the

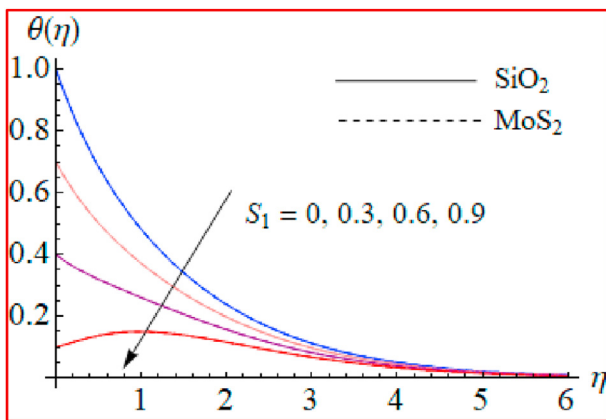


Fig. 5 –  $S_1$  versus  $\theta(\eta)$ .

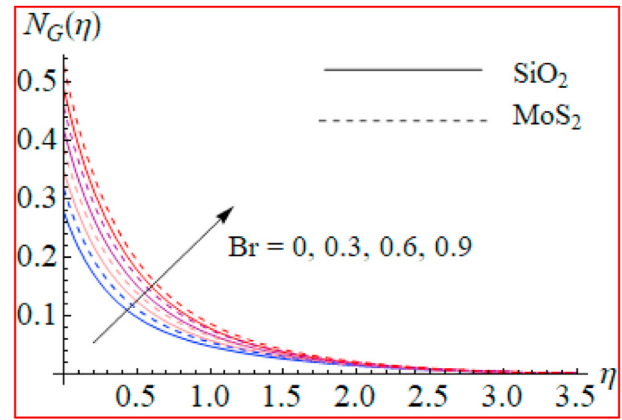


Fig. 8 –  $Br$  versus  $N_G(\eta)$ .

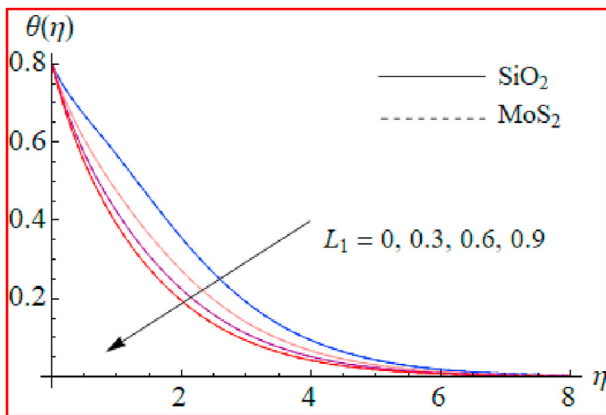


Fig. 6 –  $L_1$  versus  $\theta(\eta)$ .

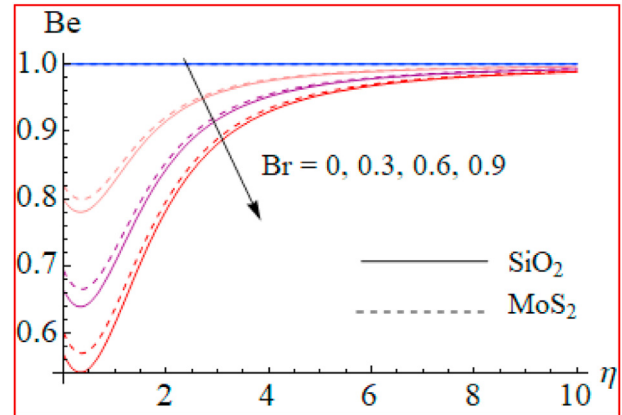


Fig. 9 –  $Br$  versus  $Be$ .

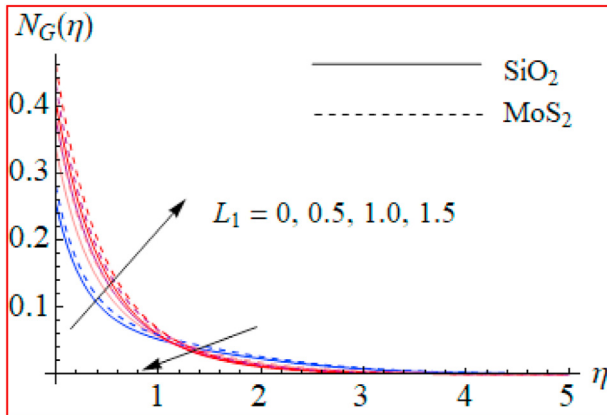


Fig. 10 –  $L_1$  versus  $N_G(\eta)$

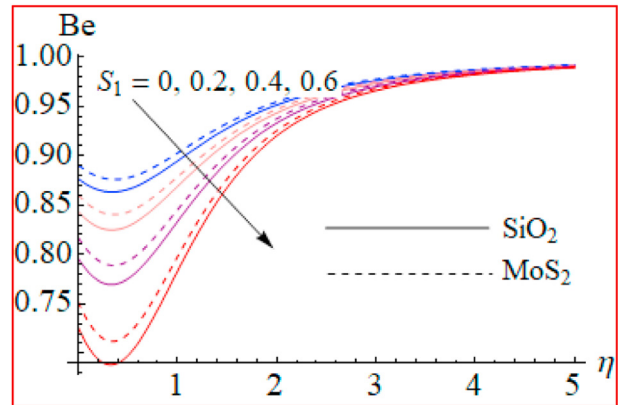


Fig. 13 –  $S_1$  versus  $Be$ .

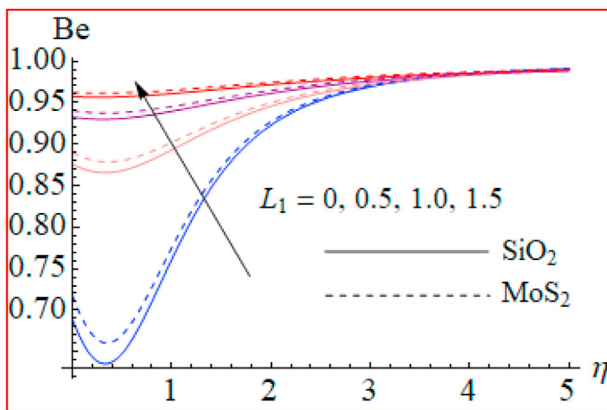


Fig. 11 –  $L_1$  versus  $Be$ .

influence of stratification parameter ( $S_1$ ) on  $(\theta(\eta))$ . Here for higher values of ( $S_1$ ) temperature difference starts increasing due to which temperature of the fluid reduces. Figs. 6 and 7 develop to show the behavior of  $(\theta(\eta))$  against ( $L_1$ ) and ( $L_2$ ) with  $SiO_2$  – water and  $MoS_2$  – water nanofluids. Since we know that there is decrease in velocity of fluid by enhancing these two parameters. So there is less disturbance in the fluid system due to increase in ( $L_1$ ) and ( $L_2$ ). In this case less resistance hence less heat produces in the system due to which temperature decays.

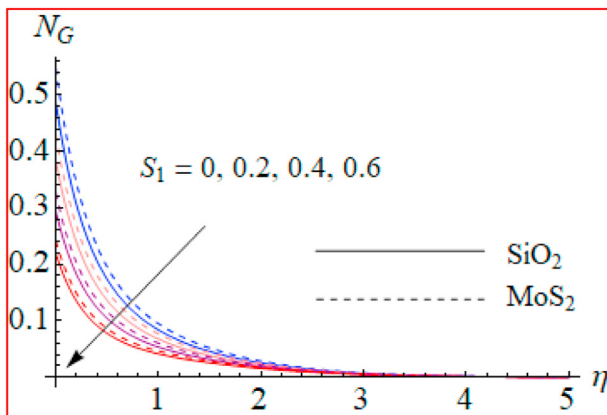


Fig. 12 –  $S_1$  versus  $N_G(\eta)$ .

### Entropy generation rate and Bejan number

Salient aspects of Brinkman number ( $Br$ ), slip parameter ( $L_1$ ) and stratification parameter ( $S_1$ ) on entropy generation and Bejan number of  $MoS_2$ -water and  $SiO_2$  – water nanofluids. Figs. 8 and 9 describe the influence of Brinkman number ( $Br$ ) on entropy generation and Bejan number for  $MoS_2$ -water and  $SiO_2$  – water nanofluids. With increasing values of ( $Br$ ) viscous dissipation irreversibility enhances due to which more resistance produces between the fluid particles hence entropy of the system boosts up. Fig. 9 shows that Bejan number is maximum at  $Br = 0$  which is equal to 1 and with increase in  $Br$  it starts decaying. Due to increase in Brinkman number ( $Br$ ) viscous dissipation irreversibility become prominent over heat transfer irreversibility. Figs. 10 and 11 are plotted to show the impact of slip parameter ( $L_1$ ) on entropy generation and Bejan number ( $Be$ ). Here entropy generation ( $N_G$ ) enhances near the surface of the sheet while shows decreasing behavior away from the sheet. Bejan number of  $MoS_2$ -water and  $SiO_2$  – water nanofluids enhances throughout the system for higher estimations of ( $L_1$ ). We can easily notice from there that entropy and Bejan number is more in case of  $MoS_2$ -water as compared to  $SiO_2$  – water nanofluid. Figs. 12 and 13 portray the impact of thermal stratification ( $S_1$ ) on entropy generation and Bejan number. Here entropy generation decays for higher values of thermal stratification parameter. With increasing values of ( $S_1$ ) temperature

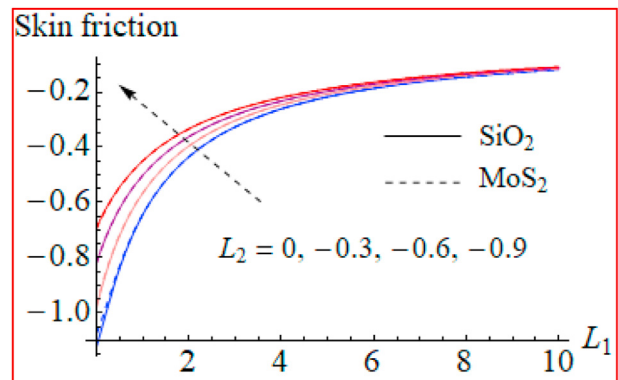


Fig. 14 – Combined analysis of  $L_1$  and  $L_2$  on skin friction coefficient.

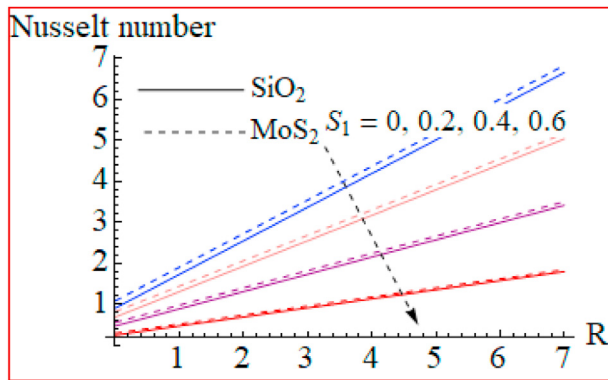


Fig. 15 – Combined analysis of  $S_1$  and  $R$  on Nusselt number.

difference starts decreasing due to which entropy decays. Fig. 13 shows that Bejan number decreases for higher values of ( $S_1$ ). Here from all figures we noticed that  $MoS_2$ -water is more as compared to  $SiO_2$  – water nanofluids.

### Physical quantities of interest

Impact of various interesting parameters ( $L_1$ ), ( $L_2$ ), ( $R$ ) and ( $S_1$ ) on skin friction and Nusselt number of  $MoS_2$ -water and  $SiO_2$  – water nanofluids is depicted in Figs. 14 and 15.

#### Skin friction coefficient

The numerical results of gradient of velocity ( $C_{fx}$ ) against first and second order slip parameters is shown in Fig. 14. Here we have noticed that by varying the values of ( $L_1$ ) and ( $L_2$ ) magnitude of skin friction coefficient decays for both  $MoS_2$ -water and  $SiO_2$  – water nanofluids.

#### Heat transfer rate

Fig. 15 elucidates the impact of radiation parameter and stratification parameter on Nusselt number for  $MoS_2$ -water and  $SiO_2$  – water nanofluids. Here Nusselt number ( $Nu_x$ ) decreases via stratification parameter while opposite impact is seen for radiation parameter.

### Conclusions

A mathematical and cost-effective numerical simulation for a two-dimensional incompressible, steady forced/mixed convective Darcy-Forchheimer nanomaterial flow towards a flat and stretched surface of sheet is addressed. The flow is electrically magnetized and saturated in the presence of magnetohydrodynamic (applied magnetic field) and Darcy Forchheimer porous medium. Entropy generation and heat transport examination of the considered problem is achieved subject to fluid friction, heat transfer and porosity or Darcy-Forchheimer porous irreversibilities through second law of thermodynamics (SLT). The obtained outcomes are verified with some fruitful and available theoretical data i.e., Shiaq et al.

[26], Golra and Sidawi [27] and Wang [28], where the comparative outcomes demonstrated the good agreement of the present computational analysis. In order to discussed the behavior of proposed problem over a stretched surface, the impacts of the Darcy-Forchheimer porous number, nanoparticle volume fraction, second order slip parameter, thermal stratification parameter in the presence of both Silicon dioxide and Molybdenum nanoparticles are graphically discussed. Some fruitful and meaningful final remarks are listed as follows:

- Among all pertinent flow parameter (Darcy-Forchheimer number, nanoparticle volume fraction, first order velocity slip, second order velocity slip, thermal stratification, Brinkman number and radiative heat flux), the behaviors of first and second order velocity slip parameters on the fluid particles velocity through permeability were more important than other parameter. The behaviors of first and second orders velocity slip parameters on the fluid field were significant and more fruitful when the particles of working materials had the capability to saturate the porous medium. On the other hand, at small liquid penetration into the permeable surface, the hydrodynamic losses were considerably affected by boundary layer approximation in both porous surface and fluid.
- Enhancing the values of nanoparticle volume fraction, the velocity of fluid particles declines.
- Increasing the thermal stratification parameter, first order velocity slip parameter and second order velocity slip parameter the thermal field and associated layer thickness declines for both Silicon dioxide and Molybdenum nanoparticles.
- The engineering quantities i.e., skin friction coefficient (surface drag force) and heat transfer rate (Nusselt number) decreases versus higher values of thermal stratification parameter and first and second order velocity slip parameters while increases via larger values of radiative heat flux for both Silicon dioxide and Molybdenum nanoparticles.
- The impact of Molybdenum nanoparticle is more prominent than the Silicon dioxide in the whole study, because the thermal conductivity of Molybdenum nanoparticle is much higher than the Silicon dioxide nanoparticle.

### Declaration of competing interest

The authors declare that they have no known competing financial interests or personal relationships that could have appeared to influence the work reported in this paper.

### REFERENCES

- [1] Hayat T, Khan MI, Qayyum S, Alsaedi A. Entropy generation in flow with silver and copper nanoparticles. *Colloid Surface Physicochem Eng Aspect* 2018;539:335–46.
- [2] Xie Z, Jian Y. Entropy generation of magnetohydrodynamic electroosmotic flow in two-layer systems with a layer of non-conducting viscoelastic fluid. *Int J Heat Mass Tran* 2018;127:600–15.

- [3] Reddy GJ, Kumar M, Anwar Beg O. Effect of temperature dependent viscosity on entropy generation in transient viscoelastic polymeric fluid flow from an isothermal vertical plate. *Phys Stat Mech Appl* 2018;51015:426–45.
- [4] Khan MI, Hayat T, Khan MI, Waqas M, Alsaedi A. Numerical simulation of hydromagnetic mixed convective radiative slip flow with variable fluid properties: a mathematical model for entropy generation. *J Phys Chem Solid* 2019;125:153–64.
- [5] Zahmatkesh R, Mohammadiun H, Mohammadiun M, Bonab MHD. Investigation of entropy generation in nanofluid's axisymmetric stagnation flow over a cylinder with constant wall temperature and uniform surface suction-blowing. *Alexandria Eng J* 2019;58:1483–98.
- [6] Khan MI, Qayyum S, Hayat T, Alsaedi A. Entropy generation minimization and statistical declaration with probable error for skin friction coefficient and Nusselt number. *Chin J Phys* 2018;56:1525–46.
- [7] Zhang D, Peng H, Ling X. Lattice Boltzmann method for thermomagnetic convection and entropy generation of paramagnetic fluid in porous enclosure under magnetic quadrupole field. *Int J Heat Mass Tran* 2018;127:224–36.
- [8] Alsabery AI, Selimefendigil F, Hashim I, Chamkha AJ, Ghalambaz M. Fluid-structure interaction analysis of entropy generation and mixed convection inside a cavity with flexible right wall and heated rotating cylinder. *Int J Heat Mass Tran* 2019;140:331–45.
- [9] Muhammad R, Khan MI, Jameel M, Khan NB. Fully developed Darcy-Forchheimer mixed convective flow over a curved surface with activation energy and entropy generation. *Comput Methods Progr Biomed* 2020;188:105298.
- [10] Barnoon P, Toghraie D, Dehkordi RB, Abed H. MHD mixed convection and entropy generation in a lid-driven cavity with rotating cylinders filled by a nanofluid using two phase mixture model. *J Magn Magn Mater* 2019;483:224–48.
- [11] Muhammad R, Khan MI, Jameel M, Khan NB. Fully developed Darcy-Forchheimer mixed convective flow over a curved surface with activation energy and entropy generation. *Comput Methods Progr Biomed* 2020;188:105298.
- [12] Bozorg MV, Siavashi M. Two-phase mixed convection heat transfer and entropy generation analysis of a non-Newtonian nanofluid inside a cavity with internal rotating heater and cooler. *Int J Mech Sci* 2019;151:842–57.
- [13] Khan MI, Qayyum S, Kadry S, Khan WA, Abbas SZ. Theoretical investigations of entropy optimization in electro-magneto nonlinear mixed convective second order slip flow. *J Magn* 2020;25:8–14.
- [14] Cho Ching-Chang. Mixed convection heat transfer and entropy generation of Cu-water nanofluid in wavy-wall lid-driven cavity in presence of inclined magnetic field. *Int J Mech Sci* 2019;151:703–14.
- [15] Khan MI, Kumar A, Hayat T, Waqas M, Singh R. Entropy generation in flow of Carreau nanofluid. *J Mol Liq* 2019;278:677–87.
- [16] Ghahremanian S, Abbasi A, Mansoori Z, Toghraie D. Investigation the nanofluid flow through a nanochannel to study the effect of nanoparticles on the condensation phenomena. *J Mol Liq* 2020;3111:113310.
- [17] Farzinpour M, Toghraie D, Mehmandoust B, Aghadavoudi F, Karimipour A. Molecular dynamics study of barrier effects on Ferro- nanofluid flow in the presence of constant and time-dependent external magnetic fields. *J Mol Liq* 2020;30815:113152.
- [18] Khan M, Malik MY, Salahuddin T, Hussain A. Heat and mass transfer of Williamson nanofluid flow yield by an inclined Lorentz force over a nonlinear stretching sheet. *Result phy* 2018;8:862–8.
- [19] Khan M, Salahuddin T, Malik MY, Mallawi FO. Change in viscosity of Williamson nanofluid flow due to thermal and solutal stratification. *Int J Heat Mass Tran* 2018;126:941–8.
- [20] Hayat T, Khan MI, Alsaedi A, Khan MI. Joule heating and viscous dissipation in flow of nanomaterial by a rotating disk. *Int Commun Heat Mass Tran* 2017;89:190–7.
- [21] Al Kalbani KS, Rahman MM, Saghir MZ. Entropy generation in hydromagnetic nanofluids flow inside a tilted square enclosure under local thermal nonequilibrium condition. *Int J Thermofluid* 2020;5:100031.
- [22] Hayat T, Khan MI, Farooq M, Alsaedi A, Waqas M, Yasmeen T. Impact of Cattaneo-Christov heat flux model in flow of variable thermal conductivity fluid over a variable thicked surface. *Int J Heat Mass Tran* 2016;99:702–10.
- [23] Nadeem S, Abbas N, Elmasry Y, Malik MY. Numerical analysis of water based CNTs flow of micropolar fluid through rotating frame. *Comput Methods Progr Biomed* 2020;186:105194.
- [24] Khan MI, Waqas M, Hayat T, Alsaedi A. A comparative study of Casson fluid with homogeneous-heterogeneous reactions. *J Colloid Interface Sci* 2017;498:85–90.
- [25] Khan M, Hussain A, Malik MY, Salahuddin T, Aly S. Numerical analysis of Carreau fluid flow for generalized Fourier's and Fick's laws. *Appl Numer Math* 2019;144:100–17.
- [26] Shaiq S, Maraj EN, Iqbal Z. Remarkable role of C3H8O2 on transportation of MoS2 - SiO2 hybrid nanoparticles influenced by thermal deposition and internal heat generation. *J Phys Chem Solid* 2019;126:294–303.
- [27] Gorla RSR, Sidawi I. Free convection on a vertical stretching surface with suction and blowing. *Appl Sci Res* 1994;52:247–57. 20.
- [28] Wang CY. Free convection on a vertical stretching surface. *J Appl Math Mech* 1989;69:418–20 (ZAMM).